DEVELOPMENT OF AN ATS™ DESIGN MODEL (ATSDEM)

Technical Rationale and Parameter Determination

Modeling of complex, expansive biological processes requires recognition that system behavior is a composite of a number of physical, chemical and biological reactions, and that each has the capability of exerting influence over the other. Within most biological treatment systems, the dominant reactions revolve around enzymatic conversion. These enzymatic reactions will influence both tissue creation and tissue reduction. The more expansive the biological system, the more difficult it becomes to identify and project the dynamics of specific reactions. For example, in modeling treatment wetlands, known as Stormwater Treatment Areas or STA, the resultant, documented removal of phosphorus was utilized to establish a general first order equation in which removal is projected, but the mechanisms involved are not individually assessed (Walker, 1995). This model, Dynamic Model for STA, or DMSTA, while quite reliable over a set period of time, projects only the rate at which phosphorus is accumulated through sediment accretion. Admittedly, it does not include efforts to model or optimize plant productivity, as noted by Walker – "*The model makes no attempt to represent specific mechanisms, only their net consequences, as reflected by long-term average phosphorus budget of a given wetland segment."*

The principle weakness of the DMSTA approach is that it presumes, and requires storage (peat accumulation), or **dA/dt > 0,** with **A** the accreted peat, and **t** is time, while assuming that there is no change in the rate factor, $\mathbf{K_e}$ **,** also know as the effective velocity, or $\mathbf{dK_e/dt = 0.}$ This relationship is incongruous with the present understanding of ecological succession, as it assumes no relationship between the collection of complex ecological processes and the accumulated stores within the ecosystem. This presumption does not eliminate the inevitability that ultimately there will be a changed ecostructure in which the mechanisms and rates of phosphorus management will change. The need recently to remove accumulated peat within a large constructed treatment wetland near the City of Orlando has validated this need for maintenance.

Within more compact intensive processes, such as activated sludge and fermentation chambers, as well as MAPS programs, greater management effort is extended towards a specific product, and typically this product is targeted specifically within the modeling efforts. For example, with activated sludge, design and operation relies upon the rate of production of the diverse population of heterotrophic and chemoautotrophic microorganisms, which collectively generate the desired oxidation and consumption of organic debris. These processes are typically compatible with the principles of ecological succession, as the accumulated biomass is removed at frequent intervals, therefore, **dA/dt = 0.** This removal stabilizes the system's dynamic, and permits long-term reliability.

MAPS, which include ATS™, are such stabilized systems that rely upon photoautrophic (green plants and certain bacteria) production, and the subsequent removal (harvesting) of accumulated production to preserve relative predictable and reliable performance. Managed photoautotrophic production of course is the basis of much of established agriculture, and has been practiced for several thousands of years—therefore it is not a new concept, and it is understandable that certain aspects of ATS™ resemble conventional farming. The difference between an ATS™ and traditional farming is oriented more around purpose than technique, although to some extent purpose directs technique. With ATS™ and other MAPS it is the intent not to maximize production for the sole purpose of food or fiber cash product generation, but rather maximizing production for the principal purpose of removal of pollutant nutrients. With an ATS™, the resultant crop value is secondary—the larger and more valuable product is enhanced water quality. In other words, algae is not grown because it fixes carbon and thereby generates a valuable product, but because in its growth, supported by the fixation of carbon, it incorporates phosphorus and nitrogen in its tissue, and thereby provides an efficient mechanism for water treatment.

As with many biological water treatment processes, the dynamics associated with the ATS™ can be described as a first-order reaction, where the rate of reaction is proportional to the concentration of

the substrate. This can be expressed through Equations 1 through 3.

$$dS/dt = -kS \qquad \text{Equation 1}$$

or

$$dS/S = -kdt \qquad \text{Equation 2}$$

Integrated between **t = 0** to **t = i** or

$$\ln(S_i/S_0) = -kt \text{ or } S_i = S_0e^{-kt} \qquad \text{Equation 3}$$

Where **S** is the nutrient concentration, **t** is time, and **k** is the rate constant

This general expression was initially applied to enzymatic reactions as described by Michaelis-Menten[19]. While the value **"k"** within the laboratory was in these vanguard studies applied to a specific substrate and a specific enzyme, the **"k"** value, as noted previously, has come to be identified within more complex biological treatment processes with the cumulative effect of a broad and fluctuating collection of reactions and organisms. While repetitive experimentation in such cases can strengthen confidence in establishing values for **"k"** on a short-term basis, it cannot, as noted previously, determine the rate of change in **"k"** as environmental conditions change within a system, such as a treatment wetland, which is not managed through tissue removal —i.e. as accretion begins to change to chemical and physical complexion of the process.

Within sustainable biological processes, in which biomass removal allows long-term stabilization of the chemical and physical environment, it is possible to orient the first-order reaction around the principal mechanism involved in nutrient removal—that being actual biomass productivity. In some cases, modeling of this productivity can target a dominant species, such as with the WHS™ technology. However, in most cases, the application of growth models is applied to a set community of involved organisms, such as with activated sludge, fixed film technology, fermentation and ATS™.

Managing a collection of organisms in this manner presents the design challenge of projecting performance of a functioning ecosystem and, in operations, manipulating parameters, to the extent practical, (e.g. hydraulic loading rate, chemical supplementation) such that the most efficient ecostructure in terms of removal of the targeted pollutant, is sustained, and thus provided a selective advantage.

When a biological unit process is oriented around sustainable community production, the first order kinetics are generally applied through the Monod[20] relationship.

$$Z_t = Z_0e^{\mu t} \qquad \text{Equation 4}$$

Where **Z** is the biomass weight and μ is the specific growth rate (1/time) when:

$$\mu = \mu_{max}S/(K_s+S) \qquad \text{Equation 5}$$

Where μ_{max} is the maximum potential growth rate and K_s is the half-saturation constant for growth limited by **S**, or the concentration of **S** when $\mu = ½\ \mu_{max}$.

Considering the flow dynamic of the ATS™, the system may be viewed as a plug flow system. Recognizing that the average biomass at any one time on the ATS™ is assumed stable **(Z_{ave})**, and relatively constant when harvesting is done frequently, and the reduction rate at steady state of **S** is also a function of the concentration of **S** within the tissue or S_t, then S_{y1} at a sufficiently small increment ***"y"*** down the ATS™ may be expressed as:

$$S_{y1} = S_{y0} - \{[S_t\{Z_{ave}e^{[\mu][(y_1-y_0)/v]} - Z_{ave}\}]/[q(y_1-y_0)/v]\} \qquad \text{Equation 6}$$

Where "**v**" is the flow velocity down the ATS™ at unit flow rate "**q**".

The conditions required for Equation 6 are that the temperature is optimal for growth, that solar intensity is relatively constant, that the process is irreversible, and that there is no inhibitory effects related to **S** within the ranges contemplated, and that the difference between S_{y1} and S_{y0} is sufficiently small down **"y"**, as to not influence μ. If temperature variations are expected, their impacts need to be considered using the classical V'ant Hoff-Arrhenius equation (Equation 7), which may be incorporated into the relationship as noted in Equations 8.

$$\mu_{opt}/\mu_1 = \Theta^{(Topt-T1)} \quad \text{or} \quad \mu_1 = \mu_{opt}/\Theta^{(Topt-T1)} \qquad \text{Equation 7}$$

Where μ_{opt} is the growth rate for given **S** at the optimal growing temperature °C, T_{opt}, and μ_1 is the growth rate for the same given **S** at some temperature °C, T_1, when $T_1 < T_{opt}$, and Q is an empirical constant ranging from 1.03 to 1.10.

$$S_{y1} = S_{y0} - \{[S_t\{Z_{ave}e^{[\mu(y1-y0)/v][1/\Theta^{(Topt-T1)}]} - Z_{ave}\}]/[q(y_1-y_0)/v]\} \qquad \text{Equation 8}$$

In more northern applications, adjustments might need to be made for light intensity as well. While there are seasonal fluctuations in Florida for both solar intensity and photoperiod, the impacts are assumed to be minimal when compared to temperature influences, and can be incorporated into the empirical determination of Θ.

Finally, if the right side of Equation 5 is included for μ, then the relationship for concentration of **S**, at the end of segment y_1 becomes Equation 9.

$$S_{y1} = S_{y0} - \{[S_t\{Z_{ave}e^{[\mu_{max}S_{y0}/(Ks+S_{y0})][(y_1-y_0)/v][1/\Theta^{(Topt-T1)}]} - Z_{ave}\}]/[q(y_1-y_0)/v]\} \qquad \text{Equation 9}$$

Estimation of μ_{max} and K_s can be done by manipulation of the Monod relationship, noted as Equation 5 to yield linear equations to which field data can be applied and plotted, as discussed by Brezonik (Monod, 1942; Brezonik, 1994). Several techniques are discussed, including Lineweaver-Burke, Hanes and Eadie-Hofstee. It is suggested that of the three methods, the Hanes method, which involves the plot of substrate concentrations **S**, as the independent variable, and the quotient of substrate concentration and growth rate, $[S]/\mu$, as the dependent variable is the preferred of the three. In such a plot, μ_{max} is represented as the inverse of the slope of the linear equation:

$$[S]/\mu = (K_s/\mu_{max}) + (1/\mu_{max})[S] \qquad \text{Equation 10}$$

Accordingly, K_s is the negative of the x-intercept, or K_s = -[S], when $[S]/\mu = 0$.

Plotting the single flow data set using the Hanes method is helpful at providing some indication of expected general range of μ_{max} and K_s. The fact that data collection, particularly as related to growth, as noted earlier, is inherently vulnerable to error, and that there are undoubtedly other factors involved in determining production rate that must be considered when deciding how to apply a developed model, and in determining the extent of contingencies included in establishing sizing and operational strategy, non-linear regression analysis, a technique beyond the scope of this review, may result in a set of parameters that provide closer projections.

The data set used in establishing the Hanes plot as shown in Table 4-1, were created from field data incorporated with the following approach:

1. Data was used for that period identified as the adjusted POR, as inclusion of results impacted

by the hurricane events, and the associated power outages represent unusual perturbations that would likely influence system performance. This POR was from May 17, 2004 to August 23, and October 23 to December 6, 2004.

2. Water loss was considered negligible down the ATS™.
3. Crop production was calculated as the mass of total phosphorus removed over the monitoring period divided by the tissue phosphorus content as % dry weight, with the tissue phosphorus content calculated using the equation note in Figure 3-7.
4. Growth rate is calculated by $\mathbf{ln(Z_t/Z_0)\ /t = \mu}$ with $\mathbf{Z_0}$, the initial algal biomass assumed to be 10 g/m^2 on a dry weight basis, adjusted to optimal growing temperature. This value is based upon a reasonable harvest of 90-95% of standing crop.
5. Optimal growing temperature (water) is set at 30^o C, with Θ= 1.10.
6. Substrate concentration is set as the mean between influent and effluent concentrations.
7. Available carbon concentration is calculated using the method described in Section 3-4.

Scattergrams of the total phosphorus, total nitrogen, available carbon, and linear hydraulic loading rate with calculated growth rate are noted in Figures 4-9 to 4-12. The patterns as seen provide indication that phosphorus influences upon growth rate are more dramatic at lower concentrations, with a "plateau" noted at high concentration indicating rather low values of $\mathbf{K_s}$. Phosphorus appears to be more influential than nitrogen or available carbon. The LHLR however, as noted previously, appears to be quite influential. This may be related to the greater available mass of nutrients per unit time, or to the influences of increased flow velocity, as discussed in a later segment of this section.

Based upon literature review and field observations, it is possible that algae productivity and nutrient removal rates are impacted by more than one parameter, particularly at low concentrations. Brezonik includes in his discussions related to Monod and diffusion algal growth dynamics the recognition that more than one controlling factor may be involved, and that the Monod relationship may need to reflect this within the model, as noted in the following equation form:

$$\mu = \mu_{max.} \{[P]/(K_p+[P])\} \{[N]/(K_n+[N])\} \{[CO_2]/(K_C+[CO_2])\} \ldots \text{Equation 11}$$

Noted in Table 4-2 are the results of Hanes plots for the four parameters considered. It is not surprising that total phosphorus shows good correlation with growth rate, as total phosphorus removal was used in calculating algae production. Nonetheless, it does appear reasonable that phosphorus is involved in growth rate determination, as noted in Figures 4-13 through 4-15. What is more difficult to explain are the negative values of $\mathbf{K_s}$, most notable during the October to December period. Initially, this might be interpreted as indication of inhibition at high concentrations. However, at these concentrations (500-1,000ppb), there is no evidence within the literature that phosphorus inhibits algae production. Rather, it appears that what may be associated with this condition is the fact that growth calculated by phosphorus uptake during this period was an underestimate of actually measured growth—see Figures 3-5 and 3-6. The implication therefore is that during this time, the system drew its phosphorus from some source other than the water column—such as stores. As discussed previously, there is little space available for such stores within an ATS™, so it is suspected that the more likely explanation for these anomalies is data error.

The relationship over the adjusted POR between LHLR and growth rate appears rather clear, as noted in Figures 4-16 through 4-18, at least within the ranges studies. The correlations shown are reasonable, even with a few "outlier" data points. As noted, the relationships associated with nitrogen and carbon are not as clear.

Table 4-1: Data set for adjusted POR

	Week ending	Period days	Average Water T C	Total P Average Concentration ppb	Total N Average Concentration mg/l	Available Carbon Average Concentration mg/l	LHLR gallons/ minute-ft	Estimated Algae Production dry grams	Calculated growth rate 1/hr
South Floway	5/17/2004	6	27.2	171	1.30	13.83	6.20	13,194	0.021
	5/24/2004	7	27.8	190	1.40	13.83	6.09	18,351	0.020
	5/31/2004	7	28.4	218	2.01	19.14	5.60	28,746	0.021
	6/7/2004*	7	29.2	178	1.90	15.24	3.90	13,681	0.015
	6/14/2004	7	27.1	116	1.70	17.98	4.41	14,627	0.019
	6/21/2004	7	30.2	106	1.48	18.56	5.62	12,103	0.013
	6/28/2004	7	31.4	75	1.49	16.23	2.69	13,488	0.012
	7/5/2004	3	32.3	57	1.70	14.07	5.12	5,277	0.018
	7/12/2004	7	31.1	72	1.30	14.07	4.44	4,094	0.007
	7/19/2004	7	30.4	48	1.19	11.90	4.82	463	0.002
	7/26/2004	7	29.4	61	1.05	12.16	4.15	6,947	0.011
	8/2/2004	7	29.5	55	1.21	22.68	4.52	6,874	0.011
	8/9/2004	7	28.3	57	0.96	11.55	3.61	4,204	0.010
	8/16/2004	5	29.7	63	1.20	22.81	5.82	6,670	0.015
	8/23/2004	7	30.4	336	2.20	30.72	3.37	18,905	0.015
	10/25/2004	7	28.0	885	1.28	25.58	5.47	6,959	0.013
	11/1/2004	7	28.3	830	2.11	11.74	2.95	3,324	0.009
	11/8/2004	7	28.2	715	2.63	26.33	6.48	3,912	0.009
	11/15/2004	7	24.8	625	1.57	25.46	4.93	5,260	0.015
	11/22/2004	7	24.3	500	2.01	21.53	4.82	2,245	0.010
	11/29/2004	7	24.7	300	1.11	17.09	4.90	16,022	0.025
Central Floway	5/17/2004	6	26.7	186	1.25	11.81	22.84	30,193	0.030
	5/24/2004	7	27.3	190	1.50	11.81	22.98	71,964	0.030
	5/31/2004	7	28.0	223	2.24	14.11	22.60	110,742	0.032
	6/7/2004*	7	29.1	178	1.90	11.27	25.11	79,193	0.026
	6/14/2004	7	27.3	129	1.79	13.54	24.55	56,162	0.029
	6/21/2004	7	30.2	119	1.53	13.35	23.40	45,956	0.021
	6/28/2004	7	30.9	88	1.54	11.98	19.14	34,307	0.018
	7/5/2004	3	31.5	65	1.26	11.17	26.51	26,807	0.036
	7/12/2004	7	30.5	77	1.30	10.37	18.30	16,849	0.015
	7/19/2004	7	30.5	48	1.15	18.04	19.57	1,910	0.005
	7/26/2004	7	29.6	67	1.10	9.88	16.96	20,676	0.017
	8/2/2004	7	30.2	66	1.19	15.47	19.52	15,628	0.015
	8/9/2004	7	28.4	58	0.96	15.62	14.21	16,114	0.018
	8/16/2004	5	29.1	70	1.12	15.76	22.72	19,803	0.025
	8/23/2004	7	30.2	346	2.21	28.94	11.78	64,722	0.023
	10/25/2004	7	27.5	880	1.28	17.65	16.47	24,019	0.022
	11/1/2004	7	27.3	815	2.05	10.59	17.97	30,617	0.024
	11/8/2004	7	27.5	710	2.17	18.03	17.22	13,906	0.018
	11/15/2004	7	24.9	630	1.81	17.82	17.14	14,583	0.024
	11/22/2004	7	23.4	490	1.94	16.00	17.03	15,984	0.028
	11/29/2004	7	24.4	335	1.09	12.84	17.33	22,940	0.029
	12/5/2004	6	23.3	240	1.52	12.84	18.16	26,852	0.040
North Floway	5/17/2004	6	27.0	171	1.25	11.66	10.52	22,410	0.026
	5/24/2004	7	27.5	210	1.60	11.66	10.71	18,990	0.020
	5/31/2004	7	28.2	223	2.19	13.99	9.56	46,102	0.025
	6/7/2004*	7	29.1	193	2.00	11.17	9.36	23,893	0.019
	6/14/2004	7	27.1	119	1.62	13.72	9.10	26,433	0.024
	6/21/2004	7	30.2	110	1.58	13.37	9.41	23,294	0.017
	6/28/2004	7	31.0	83	1.54	12.09	8.78	16,184	0.014
	7/5/2004	3	32.1	58	1.22	11.07	19.10	15,493	0.028
	7/12/2004	7	31.1	68	1.25	10.04	4.70	10,084	0.011
	7/19/2004	7	30.8	41	1.11	17.55	9.56	5,363	0.009
	7/26/2004	7	30.1	59	1.05	9.80	9.40	14,860	0.015
	8/2/2004	7	29.6	55	1.16	14.86	8.09	13,400	0.015
	8/9/2004	7	28.3	53	0.96	15.31	8.10	9,813	0.015
	8/16/2004	5	29.7	81	1.20	15.76	6.66	3,035	0.010
	8/23/2004	7	30.4	326	2.10	29.99	2.23	11,409	0.013
	10/25/2004	7	27.8	630	1.28	18.05	7.99	16,982	0.019
	11/1/2004	7	27.8	582	2.23	10.86	8.79	17,389	0.019
	11/8/2004	7	28.0	524	2.26	18.47	7.22	13,229	0.017
	11/15/2004	7	24.5	468	1.58	17.95	9.01	17,174	0.026
	11/22/2004	7	24.9	398	1.85	16.01	9.11	18,348	0.026
	11/29/2004	7	24.6	325	1.08	12.60	9.24	17,264	0.026

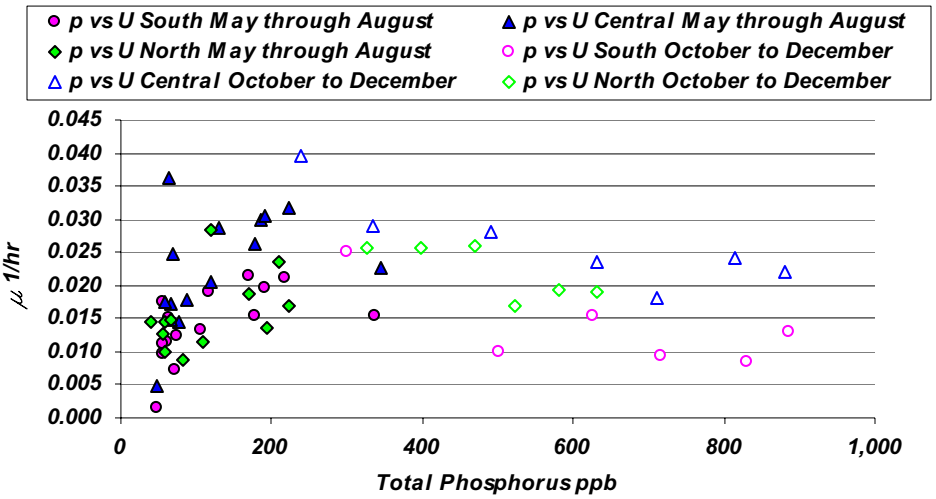

Figure 4-9: Total phosphorus Vs. calculated growth rate adjusted POR data set

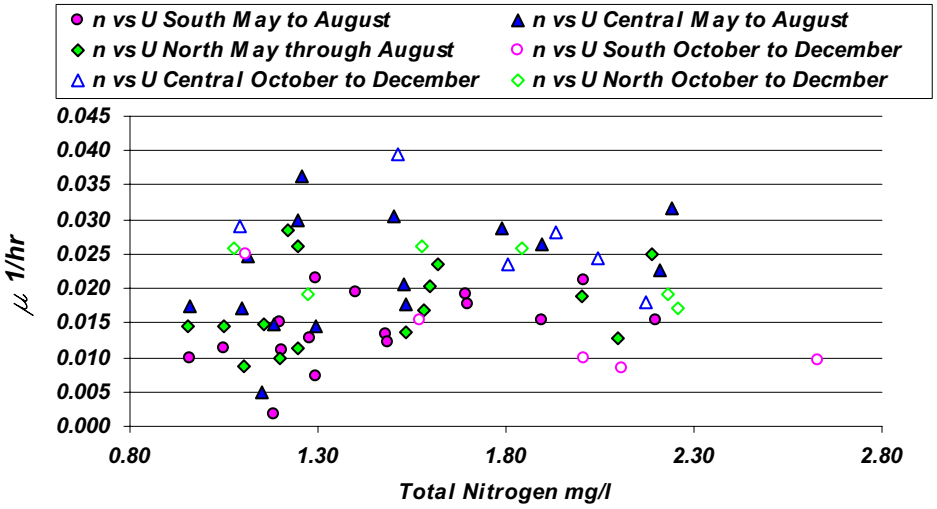

Figure 4-10: Total nitrogen Vs. calculated growth rate adjusted POR data set

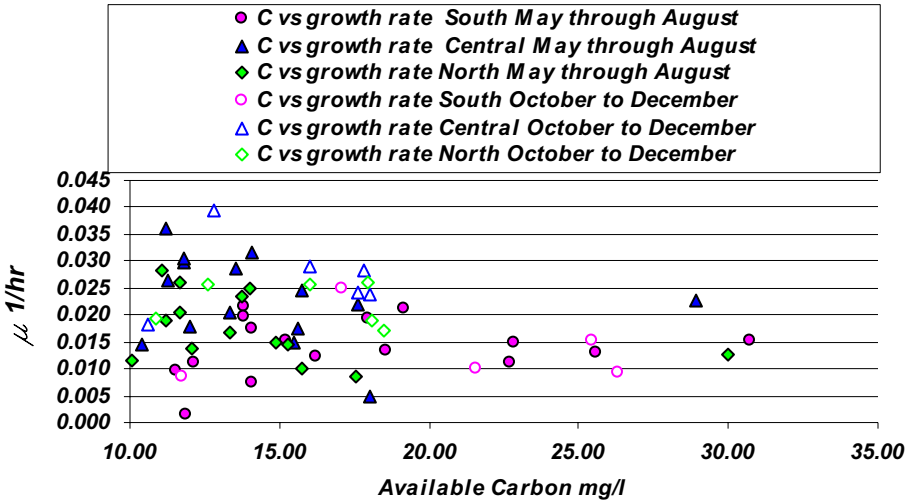

Figure 4-11: Available Carbon Vs. calculated growth rate adjusted POR data set

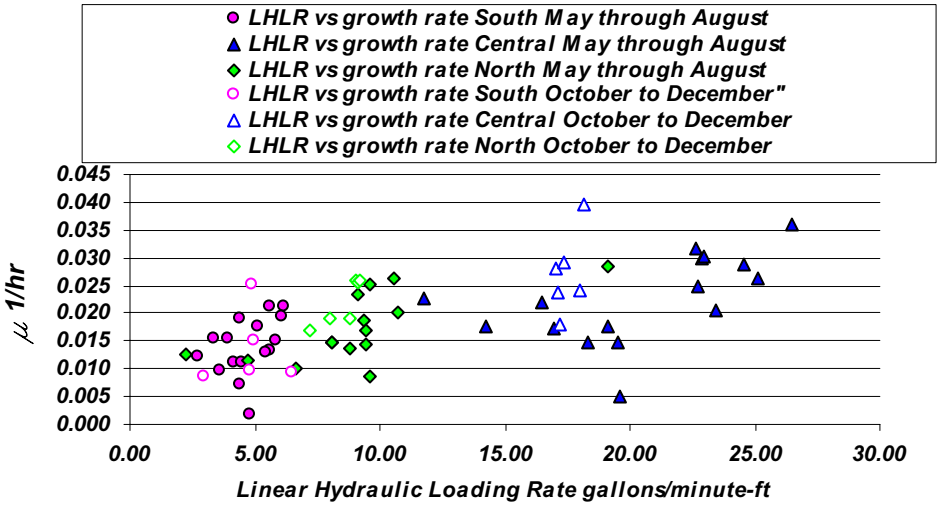

Figure 4-12: Linear Hydraulic Loading Rate Vs. calculated growth rate adjusted POR data set

Table 4-2: Results of Hanes analysis

Floway	Time Period	Parameter	r^2	$\mu_{max\ 1/hr}$	K_s *
Combined	Total POR	TP	0.720	0.015	-15
Combined	May through August	TP	0.327	0.025	71
Combined	October to December	TP	0.740	0.015	-81
Combined	Total POR	TN	0.021	0.031	1.72
Combined	May through August	TN	0.002	-0.091	-11.04
Combined	October to December	TN	0.536	0.017	-0.32
Combined	Total POR	Available C	0.126	0.014	-0.27
Combined	May through August	Available C	0.078	0.016	3.16
Combined	October to December	Available C	0.590	0.013	-5.17
Combined	Total POR	LHLR	0.159	0.030	8.6
Combined	May through August	LHLR	0.147	0.029	9.5
Combined	October to December	LHLR	0.805	0.037	5.7

*** ppb for TP, mg/l for TC and Carbon, gpm/ft for LHLR**

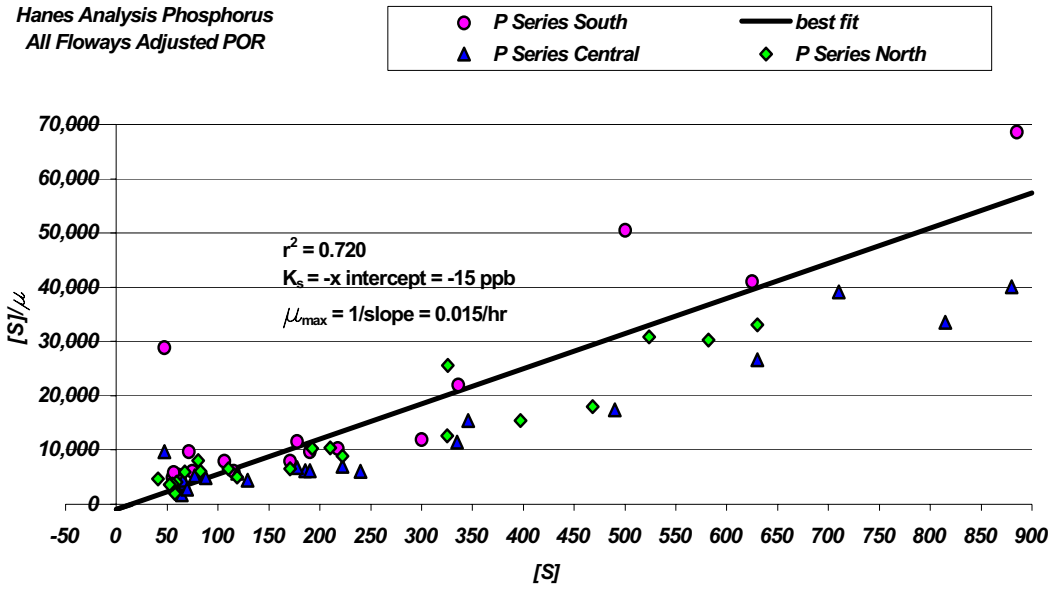

Figure 4-13: Hanes plot total phosphorus all floways over adjusted POR

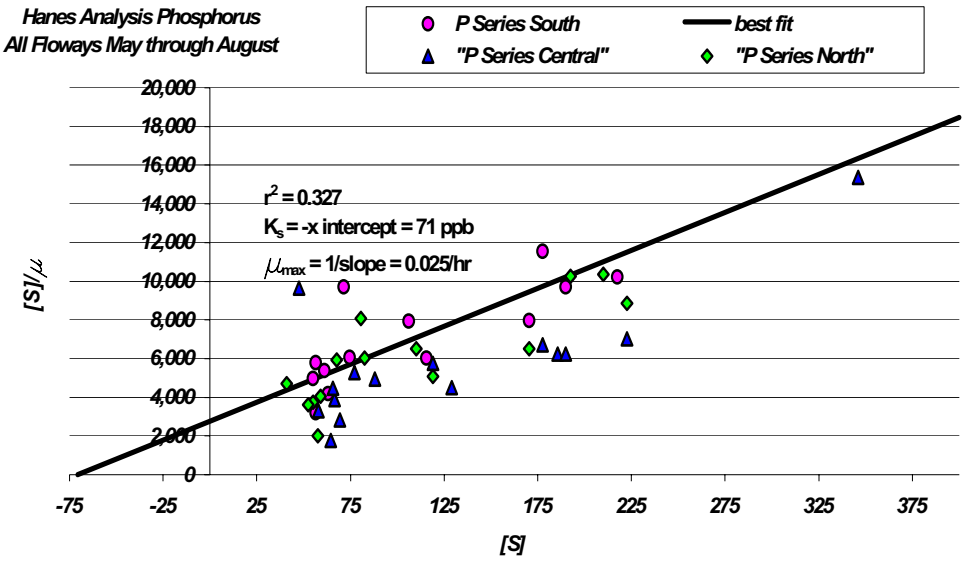

Figure 4-14: Hanes plot total phosphorus all floways May through August

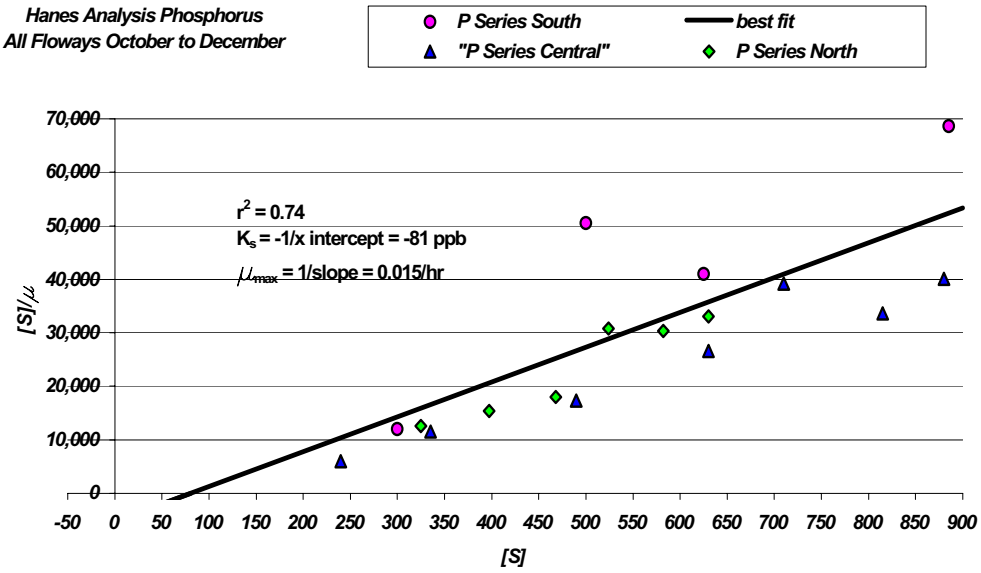

Figure 4-15: Hanes plot total phosphorus all floways October to December

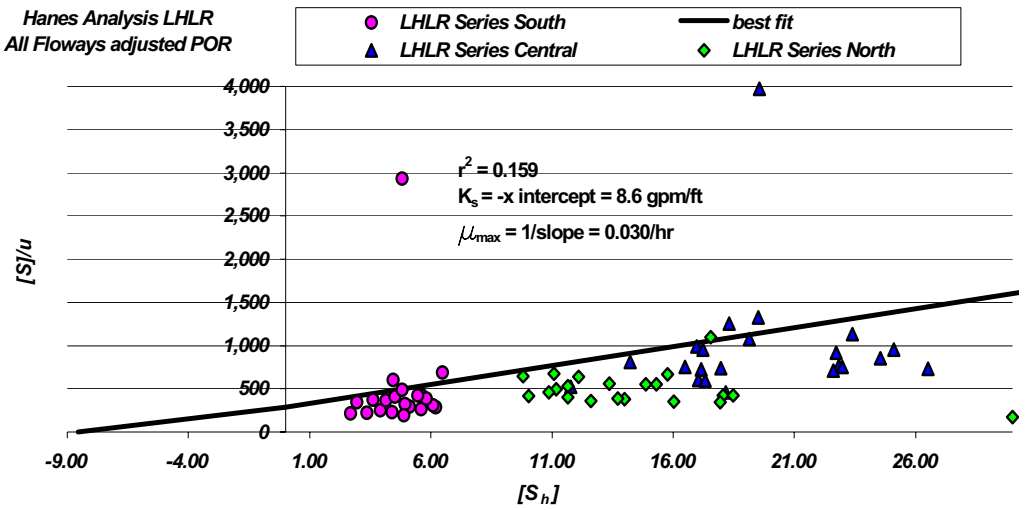

Figure 4-16: Hanes plot LHLR all floways over adjusted POR

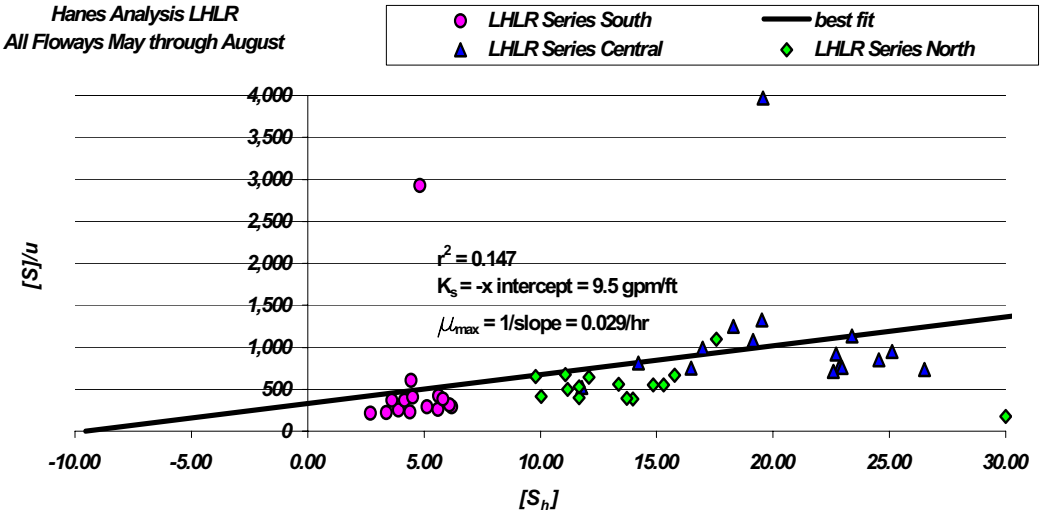

Figure 4-17: Hanes plot LHLR all floways May through August

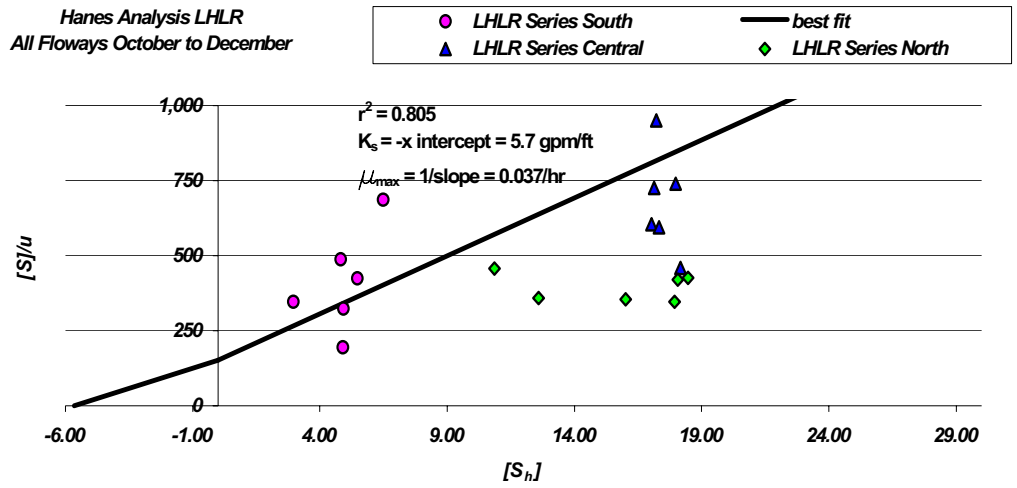

Figure 4-18: Hanes plot LHLR all floways October to December

The issue of the influence of flow rate and velocity upon algae growth rate has been extensively reviewed within the literature. In a detailed discussion regarding the relative role of nutrient uptake within algae as influenced by both Monod dynamics and boundary layer transport through molecular diffusion, Brezonik presents work done on models that include consideration of both phenomena. He notes that at high substrate [S] concentrations, boundary-layer diffusion control over growth rate becomes negligible. At low concentrations, however, diffusion influences can overwhelm the Monod kinetics, and uptake projections based solely upon the Monod growth equations without inclusion of diffusion influence can be higher than observed. He identifies a factor **1/(1+P')** as representative of the proportion of the total resistance to nutrient uptake caused by diffusion resistance, where:

$$P' = a(14.4\pi D_s r_c K_s)/V \qquad \textbf{Equation 12}$$

When ***a*** = shape factor applied to algal cell shape

D_s = Fick's diffusion coefficient as substrate changes per unit area per unit time

r_c = algal cell radius

K_s = Substrate concentration when uptake rate ***v*** is ½ of maximum uptake rate ***V***

V = Michaelis-Menten substrate uptake rate mass per unit time

The Michaelis-Menten ***V*** may be seen in this case as analogous to the Monod maximum growth rate or μ_{max}, therefore it is reasonable to express the equation as:

$$P' = a(14.4\pi D_s r_c K_s)/\mu_{max.} \qquad \textbf{Equation 13}$$

Brezonik includes this P' into the Monod relationship at low concentrations of S, resulting in the equation:

$$\mu = \mu_{max.}\ [P'/(P'+1)]S/\ K_s \qquad \textbf{Equation 14}$$

It is noted then, the smaller P' the greater the influence of growth.

Observations regarding velocity influences relate to the general thickness of the boundary layer around the cell wall (Carpenter et al., 1991). This is consistent with discussions offered by Brezonik who notes that "*turbulence increases nutrient uptake rates at low concentrations where diffusion limitations can occur*". He generally observed that at low concentrations Monod dynamics can be influenced by boundary layer conditions, and uptake rates may be lower than predicted by Monod kinetics. This is relevant when discussing the use of periphytic algae for reduction of total phosphorus to low concentrations, because passive systems such as PSTA, which rely upon extensive areas and very low velocities, would be expected to be much more restrained by boundary layer thickness at low concentrations which is inversely related to the gradient through which diffusion occurs (Carpenter et al., 1991; Brezonik, 1994). The ATS™ system, by adding the influence of flow and turbulence can substantially enhance the uptake rate and production of the algal turf.

Turbulence and water movement therefore serve to increase the rate of substrate transport, and hence decrease the importance of diffusion. This quite logically is why the use of high velocities and turbulence (e.g. oscillatory waves) enhances algal nutrient uptake. In low nutrient conditions there exists a minimum velocity (u_{min}) at which diffusion limitation of nutrient uptake is avoided. This is defined mathematically as:

$$u_{min} = (2D_s/r_c)\{(2/P')-1\} \qquad \text{Equation 15}$$

This means that at P' = 2, u_{min} = 0, and u_{min} increases as P' decreases. Values for P' of some algae species are provided, ranging from 0.33 to 680, but there is no discussion offered for assessing the cumulative influence of an algal turf community upon the general role of diffusion or how u_{min} might be determined on the ecosystem level. Rather, empirical information such as that provided by Carpenter et al. and work such as that done on the single-stage ATS™ floways can provide insight into the reaction of algal communities to velocity changes.

It is noteworthy that at low nutrient concentrations, adapted algae species would likely be characterized by a low K_s value. This is validated by Brezonik, who notes the difficulty in determining the controlling influence of nutrients upon algae production at low nutrient levels, as "*K_s may be below analytical detection limits—making it difficult to define the μ vs. [S] curve*." He includes some of the documented K_s values for several algae species associated with low nutrients. Phosphate appears as a limiting nutrient in several cases, with K_s values as low as 0.03 μM as PO_4, or about 3 ppb as PO_4, or just less than 1 ppb as phosphorus. As K_s is directly proportional to P', then it would not be unexpected that at low nutrient levels, P' would be comparatively small, and hence u_{min} comparatively large—the implication being that elimination of diffusion influence becomes very important, and hence flow velocity becomes an important design parameter. As noted, Kadlec and Walker made reference to the influence of flow velocity upon the efficacy of PSTA systems. With velocities orders of magnitude greater within ATS™ systems, it becomes an even more essential design component with ATS™. The inclusion of higher velocities and oscillatory motion within the ATS™ operational protocol allows contemplation of much higher phosphorus uptake rates, which has broad economic implications.

One practical way to include flow in an operational model, is to treat LHLR as a controlling parameter. It seems appropriate then to consider a growth model, in which two factors are included in the Monod equation (see Equation 10). It is then reasonable to include both total phosphorus and LHLR in the case of this dataset. The parameters $\mathbf{K_s}$ and μ_{max} can then be approximated through convergence to the lowest standard error between actual and projected total phosphorus concentration. Once the parameters are so calibrated with the Central Floway data, then the model reliability can be tested with data from the North and South Floways. This was done, applying the following relationship, as modified from Equation 9:

$$\mathbf{S_{pp} = S_{pi} - \{[S_t\{Z_o e^{\mu max\,[(S_{pa}/(Ksp+S_{pa})]\,[(Lp/(Khp+Lp))[24t]\,[1/\Theta^{(Topt-T1)}} - Z_o\}]/V_p\}} \qquad \textbf{Equation 16}$$

Where S_{pp} = projected effluent total phosphorus concentration for sampling period

$\mathbf{S_{pi}}$ = Influent total phosphorus concentration for sampling period

$\mathbf{Z_o}$ = Initial algal standing crop at beginning of sampling period

$\mathbf{S_{pa}}$ = Mean total phosphorus concentration across ATS™ for sampling period

$\mathbf{K_{sp}}$ = Monod half-rate coefficient total phosphorus

$\mathbf{L_p}$ = Linear Hydraulic Loading Rate for sampling period

$\mathbf{K_{hp}}$ = Monod half-rate coefficient LHLR

t = sampling period time in days

$\mathbf{V_p}$ = Volume of flow during sampling period

The result of the calibration run for the Central floway is shown in Table 4-3 and Figure 4-19. The parameter set which resulted in the best projection (lowest standard error=40.61 ppb) was μ_{max} = 0.04/hr, $\mathbf{K_{sp}}$ = 37 ppb, $\mathbf{K_{hp}}$ = 9.3 gpm/ft, $\mathbf{T_{opt}}$ = 29.9 °C and Θ = 1.10, with an initial standing crop of 10 dry-g/m^2.Using these values, the model was applied to the other two floways, as noted in Figures 4-20 and 4-21.

Table 4-3: ATSDEM Projection effluent total phosphorus Central Floway

$Z_{0\ dry}$-g	1390
Θ	1.10
T_{opt} °C	29.9
K_{sp} ppb	37
K_{sh} gpm/ft	9.30
μ_{max} 1/hr	0.04

	Week ending	Period days	Average Water Temperature C	Period Flow gallons	Sp Average P ppb	Sh LHLR gpm/ft	Estimated P tissue Content	Field Calculated Growth Rate	Projected Growth Rate	Influent Total P ppb	Effluent Total P ppb	Projected Total P
Central	**5/17/2004**	**6**	26.7	986,787	186	22.8	0.63%	0.026	0.017	211	160	184
	5/24/2004	**7**	27.3	1,204,631	190	23.0	0.63%	0.028	0.019	240	140	197
	5/31/2004	**7**	28.0	1,157,989	223	22.6	0.65%	0.030	0.020	305	140	245
	6/7/2004	**7**	29.1	1,139,115	178	25.1	0.63%	0.028	0.022	235	120	151
	6/14/2004	**7**	27.3	1,265,598	129	24.6	0.60%	0.026	0.018	164	94	133
	6/21/2004	**7**	30.2	1,237,320	119	23.4	0.59%	0.025	0.022	148	90	74
	6/28/2004	**7**	30.9	1,179,360	88	19.1	0.57%	0.023	0.021	110	66	53
	7/5/2004	**3**	31.5	964,656	65	26.5	0.56%	0.051	0.022	85	44	77
	7/12/2004	**7**	30.5	572,540	77	18.3	0.57%	0.019	0.019	99	55	15
	7/19/2004	**7**	30.5	922,204	48	19.6	0.55%	0.008	0.016	49	46	19
	7/26/2004	**7**	29.6	986,135	67	17.0	0.56%	0.020	0.016	82	51	53
	8/2/2004	**7**	30.2	854,905	66	19.5	0.56%	0.019	0.018	79	52	34
	8/9/2004	**7**	28.4	983,700	58	14.2	0.55%	0.019	0.013	70	46	54
	8/16/2004	**5**	29.1	716,421	70	22.7	0.56%	0.028	0.017	90	49	70
	8/23/2004	**7**	30.2	817,852	346	11.8	0.73%	0.027	0.021	422	270	317
	10/25/2004	**7**	27.5	830,325	880	16.5	1.05%	0.021	0.020	920	840	801
	11/1/2004	**7**	27.3	905,817	815	18.0	1.01%	0.023	0.020	860	770	754
	11/8/2004	**7**	27.5	867,933	710	17.2	0.95%	0.018	0.020	730	690	626
	11/15/2004	**7**	24.9	864,060	630	17.1	0.90%	0.018	0.015	650	610	605
	11/22/2004	**7**	23.4	858,542	490	17.0	0.81%	0.019	0.013	510	470	483
	11/29/2004	**7**	24.4	873,224	335	17.3	0.72%	0.021	0.014	360	310	332
	12/5/2004	**6**	23.3	784,534	240	18.2	0.66%	0.026	0.012	270	210	255

Mean TP Effluent actual ppb	**242**
Mean TP Effluent projected ppb	**251**
Standard error of estimate ppb	**40.61**

The model displayed reasonable, and conservative projections, and may be considered applicable for initial sizing of proposed facilities. Depending upon the level of performance demand placed upon the facility, the design engineer may want to include a contingency factor to cover the standard error, which ranged from 17% to 35%. Considering that the difference between the actual and projected mean effluent concentrations for the POR were so close, it is concluded that for long-term projections, the ATSDEM model is suitable for ATS™ programs that fall within the general water quality and environmental ranges studied. In some cases, particularly if there are significant differences in conditions, or when performance tolerances are small, “bench” scale testing may be a recommended pre-design exercise.

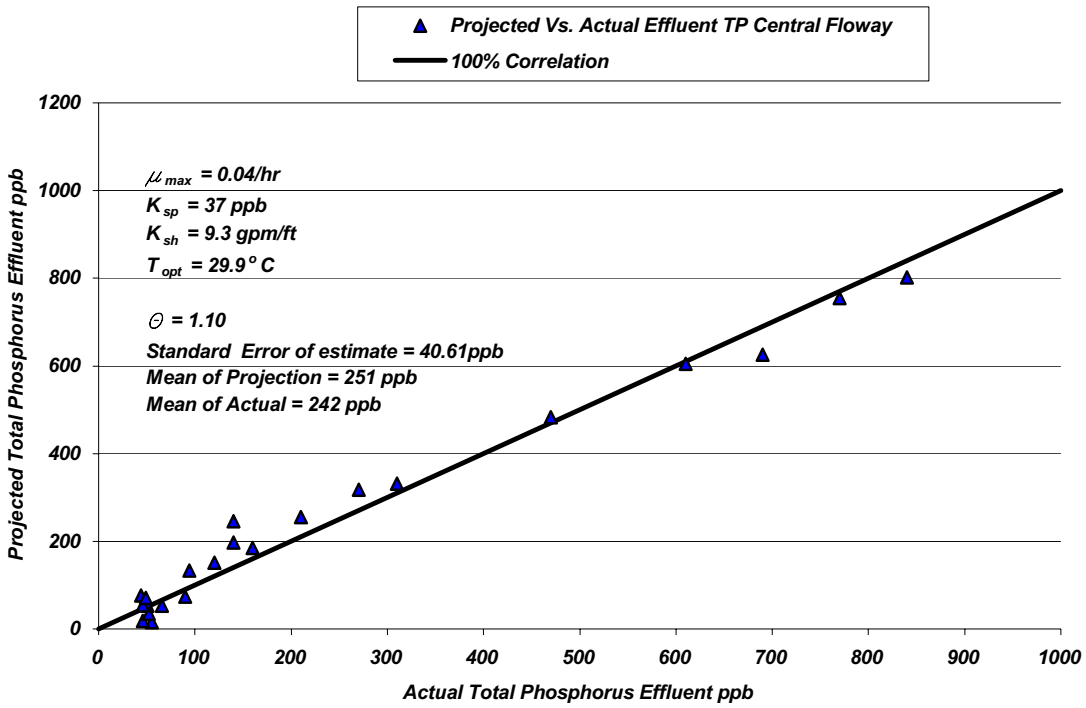

Figure 4-19: Actual Vs. ATSDEM Projected total phosphorus effluent concentration Central Floway

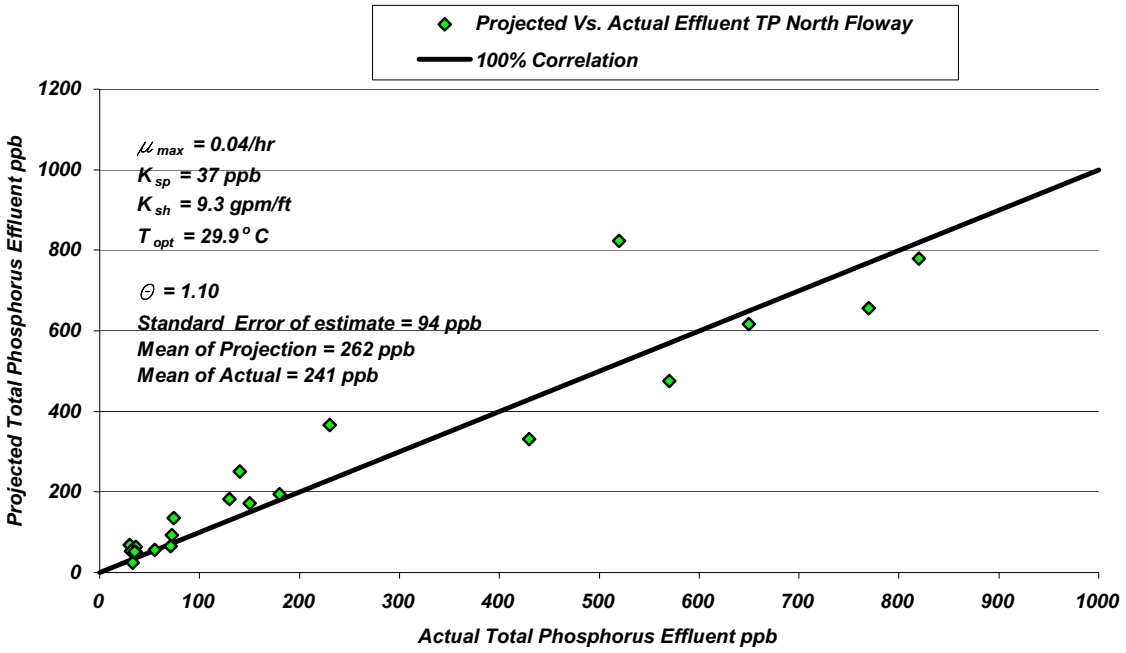

Figure 4-20: Actual Vs. ATSDEM Projected total phosphorus effluent concentration North Floway

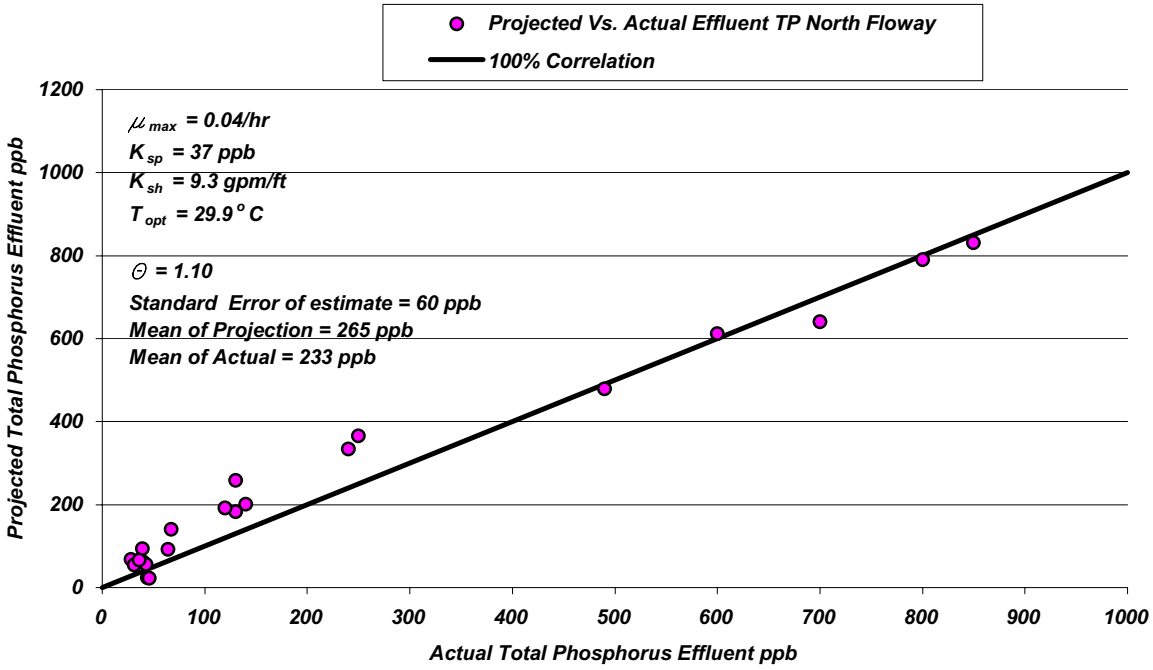

Figure 4-21: Actual Vs. ATSDEM Projected total phosphorus effluent concentration South Floway

While models such as ATSDEM are helpful in conducting conceptual level sizing of a proposed facility, and the various components associated with the proposed facility, and for projecting the rate of production and the harvesting needs, they assume that system operation is conducted such that the design provisions are sustained. As with most biological systems, the ultimate success and efficiency of a system relies heavily upon effective operational management, and the ability of a skilled operator to recognize, and sustain a healthy working biomass.

A Practical EXCEL Spreadsheet based ATSDEM

While very complex computer models could certainly be developed for sizing and designing ATS™ systems, a practical EXCEL spreadsheet model is often the most helpful to the engineer at the conceptual and preliminary engineering level, and may well be all that is required, as long as design conditions are relatively predictable, and within ranges for which the model is developed, and the engineer includes sufficient contingency provisions to allow operational flexibility. The general theory of function regarding ATS™ has already been described, with Monod growth kinetics, and diffusion boundary influences both incorporated into the basic algorithm. The basic premise for ATS™ is that 1) it is driven by photosynthesis, or primary productivity, and that sustaining high levels of productivity through frequent harvesting is essential and 2) the principal mechanism for removal of nutrients through an ATS™ is direct plant uptake, either through incorporation into tissue, luxury storage within cellular organelles, or precipitation/adsorption upon the cell wall.

Before proceeding with the refinement of a practical EXCEL based model, it is crucial that those involved in sizing and design, be even more sensitive to the importance of operational efficiency, as mentioned in the previous section. The modeling includes assumptions that the system is harvested effectively and completely, with biomass removal complete, and that the standing biomass is sustained at a density that prevents senescence or excessive necrosis. It has been observed that incomplete or too infrequent harvesting can interfere with performance. Harvesting at improper frequencies can also result in excessive densities and attendant poor performance. The general operational strategy is to maintain a consistent biomass range on the ATS™ at all times, and the modeling is based on the presumption that this is done. Senescent algae resulting from improper harvesting strategy will interfere and compete with the uptake of water column associated nutrients, as they become a rudimentary “soil” for new plant communities—such as aquatic vascular plants, and pioneer transitional plants (e.g. Primrose willow and cattails). This new ecostructure becomes less dependent upon the water column as its nutrient source, which accordingly will retard performance. It is a critical operational component then that harvesting be used to “pulse stabilize” the ecosystem, and thereby avoid successional pressures. This general strategy is the foundation of all MAPS technologies, as well as heterotrophic based systems, such as activated sludge.

It is typical that the harvesting frequency for an ATS™ in warm season conditions will be about every seven days, meaning that the entire ATS™ floway is completely harvested every seven days. In the cooler season, this frequency will typically increase to about a 14 day cycle. ATSDEM projections are based upon a composite average condition for the entire floway. For example a mean standing biomass, Z_{ave} represents the standing crop at anytime as dry-g/m^2 averaged over the whole ATS™ area. It is a function of the frequency of harvesting, and can be estimated through Equation 17.

$$Z_{ave} = \left(\sum_{m=1}^{n} Z_0 e^{24 m \mu} \right) \Big/ n$$

Equation 17

Where **m** is the days since harvest, and **n** is the days between harvests. While setting the optimal value of Z_{ave} will ultimately be by the operator, it may be expected to be higher in warmer months, perhaps over 160 dry-g/m^2, while in the cooler months it may be difficult to establish a crop over 75 dry-g/m^2.

It is recognized that any one section of the ATS™ may be providing better or less treatment than the model projection, but as an average, the model effluent estimate and actual composite effluent can be expected to be similar. This applies to any time period during the operation. While photosynthesis occurs only during the daytime, productivity projections are based upon a 24-hour period, as experience indicates that nutrient uptake continues with the loss of sunlight, even if carbon fixation is discontinued.

While the model is based upon the assumption that direct nutrient uptake within the plant biomass is the sole removal mechanism, under certain conditions other phenomenon may also contribute—including luxury uptake; adsorption; emigration through invertebrate pupae emergence and predation; and chemical precipitation, both within the water column directly, and upon the surface of the algal cell wall. Some evidence of these factors is noted with the change in tissue phosphorus concentration with change in water column total phosphorus concentration, as noted previously. By incorporating the change in phosphorus concentration within the tissue, it is presumed that ATSDEM incorporates the influence of these other phosphorus removal mechanisms.

In the case of an ATS™, the flow parameter is expressed as gal/minute-ft of ATS™ width, also known as the Linear Hydraulic Loading Rate or LHLR, as presented previously. The LHLR as discussed previously is incorporated into the ATSDEM equations. The LHLR converts to flow by multiplying by the ATS™ width. Width in this case does not refer to the short side of a rectangle, but rather the length of the influent headwall in which the flow is introduced to the ATS™. In actuality this "width" may well be larger than the ATS™ "length", which is the distance from the headwall to the effluent flume. Within the ATS™ velocity can be estimated using the Manning's Equation:

$$V = (1.49/n)r^{2/3}s^{1/2}) \qquad \textbf{Equation 18}$$

Where **V** = velocity fps
n = Manning's friction coefficient
r = hydraulic radius = flow cross- section area/wetted perimeter
s = floway slope

However, the Manning's coefficient "**n"** will vary as the algal turf develops, and is harvested, and in addition, surging will create a predictable change in flow from nearly zero to something greater than u_{min} (Equation 15*)* during the siphon (surge) release. Actual velocity variations are best determined from field observations under different conditions (e.g. high standing biomass, pre-surge, post surge, etc.)

As applied to an ATS™, the Manning Equation can be simplified by first multiplying both sides of the equation by the flow area A, which is equal to the flow depth (d) in feet times the ATS™ width (w) in feet, or:

$$Q_{cfs}=Vdw = (1.49/n)dw)r^{2/3}s^{1/2} \qquad \textbf{Equation 19}$$

As the hydraulic radius r is flow area (A) over the wetted perimeter, then:

$$r = dw/(w+2d) \qquad \textbf{Equation 21}$$

Therefore:

$$Q_{cfs} = 0.00223(LHLR)w \qquad \textbf{Equation 22}$$

when **LHLR** is gallons/minute-ft. If **w** is set at 1 ft, then

$$LHLR = \{0.00332d^{5/3}s^{1/2}\}/[n(2d+1)^{2/3}] \qquad \textbf{Equation 23}$$

This allows for the flow depths to be established for specific Manning's "n" values and slopes, and accordingly, velocity can be estimated. These relationships are noted in Figure 4-21.

As noted, the higher the floway slope, the greater flexibility in terms of maintenance of a critical velocity—i.e. the velocity at which boundary layer disruption is complete. However, higher slopes require greater earthwork quantities and higher lifts.

Down a floway then, the change in phosphorus concentration (dS_p/dt) may be expressed as:

$$\mathbf{dS_p/dt = S_t(dZ/dt)/ q_t} \qquad \textbf{Equation 24}$$

Where $\mathbf{q_t}$=control volume over time increment

The change in floway length traversed by the control volume, with time, **dL/dt**, is expressed as:

$$\mathbf{dL/dt = vt} \qquad \textbf{Equation 25}$$

These relationships hold for a relatively short time sequence when $\mathbf{S_{t0} \sim S_{t1}}$, e.g. one second. This then can be put into a spreadsheet to facilitate assessment of ATS™ performance using Equation 8 adjusted per Equation 15, under established $\mathbf{K_s}$ and μ_{max} values. The Manning relationship is incorporated into the model to allow estimation of Velocity and average flow depth.

The actual format for the ATSDEM spreadsheet model includes a front-end tutorial sheet, followed by a Design Parameter and Summary Worksheet, followed by a Z_{AVE} worksheet, and finally the Model Run Worksheet. These are presented within Appendix A.

The example used for the model run is for a proposed 300 ft long ATS™ system located in the Lake Okeechobee Watershed with a flow of 25 MGD, a design LHLR of 20 gallons/minute-ft, requiring a width of 868 feet and a process area of 5.98 acres. At an incoming total phosphorus concentration of 150 ppb, and evaluating the proposed facility over four quarters, using water temperature from existing field data, the annual total phosphorus removal, as noted in Table 4-4, is 3,149 lbs/year, with an annual harvest of 4,140 wet tons, resulting in the generation of 561 cy of finished compost. A typical model summary printout is noted for Quarter 2 in Figure 4-22.

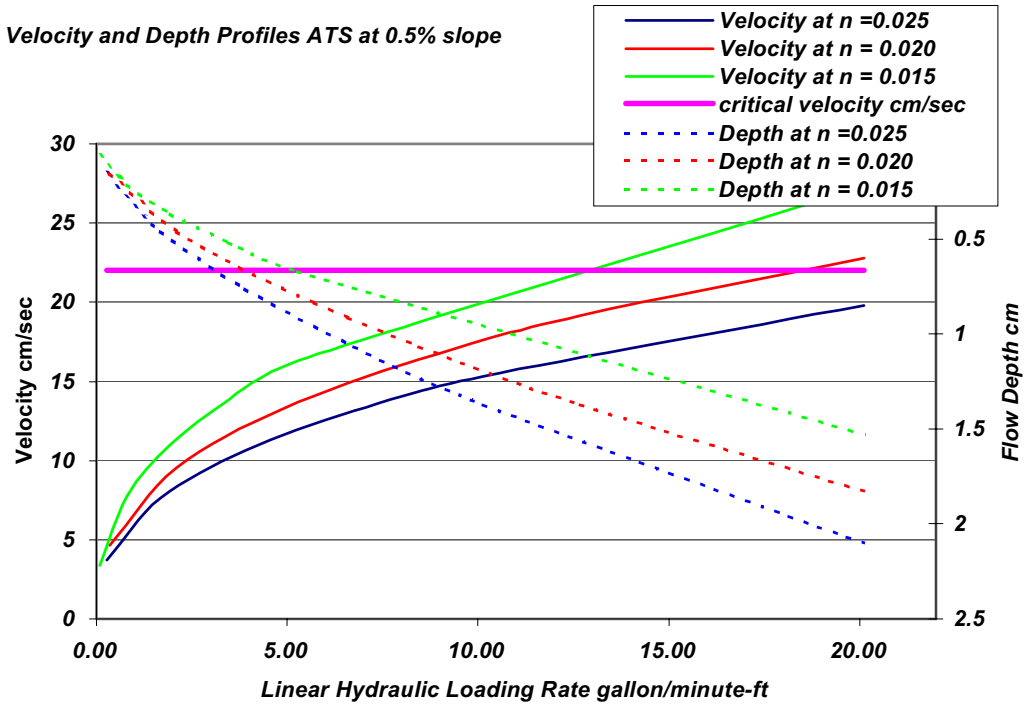

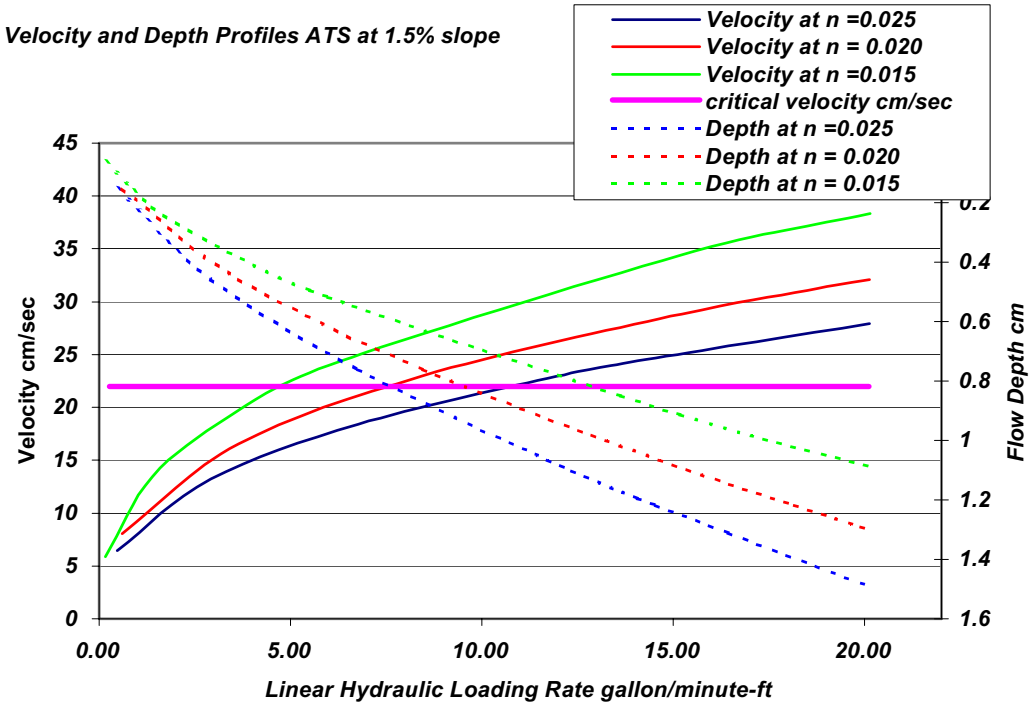

Figure 4-21: Velocity, LHLR and depth relationships as determined from Manning Equation

Table 4-4: ATSDEM summary 25 MGD Lake Okeechobee Watershed ATS™

Conditions:	
Flow MGD	25
Average Flow Velocity fps	0.93
Average Flow Depth inches	0.58
Average Flow-through time minutes	324
Influent TP	150
ATS length ft	300
ATS Headwall Width ft	868
ATS Acreage	5.98
ATS slope	1.00%

Parameter	Q1	Q2	Q3	Q4	Total Annual
Effluent Total Phosphorus ppb	133	109	74	118	109
Total Phosphorus Areal Removal Rate lb/acre-yr	212	524	970	401	527
Total Phosphorus Removed lb	317	783	1,450	599	3,149
Wet Harvest tons	532	83	2,510	1,015	4,140
Compost tons	33	83	157	63	337
Compost CY	55	139	261	106	561

Panel A Velocity Conditions

Floway slope (s)	Manning n	Manning Factor (1)	Manning Factor (2) Match	LHLR gpm/lf	LHLR cfs/lf	LHLR liters/sec-lf	Average flow depth (d) ft	Velocity fps	Flow length interval ft
0.01	0.02	0.005981	0.005981	20	0.045	1.280	0.05	0.93	0.93

Panel B Process Conditions

Water T °C	Optimal T °C	Θ	K_{sp} as ppb TP	K_{sh} as LHLR gpm/ft	μ_{max} 1/hr	S_o ppb Total P	Harvest Cycle days	Z_{ave} dry-g/m^2	Z_0 dry-g/m^2	S^*_p Total Phosphorus ppb
27.44	29.9	1.10	37	9.3	0.04	150	7	105.74	10.00	30

Panel C Performance

Control Time Seconds	Control Volume liter	Final Total P S_f ppb	Total Flow Time seconds	Total P percent removal	Floway Length ft	Areal Loading Rate TP g/m2-yr	Areal Loading Rate TP lb/acre-year	Areal Removal Rate TP g/m2-yr	Areal Removal Rate TP lb/acre-yr	Average Production dry-g/m^2-day	Area per time sequence m^2
1	1.280	109	324	27%	300	214	1909.18	59	524.07	27.39	0.086

Panel D System Design

Total Flow mgd	Floway Width ft	Floway Area acres	Total P removed lb/period	Moisture % wet harvest	Moisture % compost	Period Wet Harvest tons	Period Dry Harvest tons	Period Compost Production wet tons	Performance Period days	μ_{ave} 1/hr
25	868	5.98	783.38	5%	40%	1,332	67	83	91.25	0.0168

Note: Inputs in Blue Print

Figure 4-22: Conceptual Design Parameter and Summary Worksheet Lake Okeechobee Watershed Quarter 2 ATS™ 25 MGD

ASSESSMENT OF HURRICANE IMPACTS

As mentioned previously, Hurricane Frances passed over the S-154 site on September 3 and 4, 2004. Based upon review of weather data, it appears that wind velocities approached 95 mph for a sustained period. Rainfall exceeded 7"—the limit of the on-site gauge—and may well have been close to 10". Sometime during this period, power was lost, and the operations terminated. The runoff associated with the heavy rainfall, combined with wind, scoured the ATS™ units, resulting in a flushing of algae solids and nutrients. Sampling was terminated with the loss of power.

After Hurricane Frances, the facility was inspected, and no significant damage was recorded. However, power remained off until the late afternoon, September 14, 2004. At that time the system was returned to operation until September 27, 2004, when the facility was hit by Hurricane Jeanne, which had associated wind and rainfall similar to Frances. The power was again lost, and did not return until October 3, 2004. Therefore the system experienced 18 days of power outage in the one-month period between September 3, 2004 and October 3, 2004. Water quality and field data for the period following Hurricane Jeanne appeared to return too normal by October 23, 2004. .

Based upon data collected from the week of August 30, 2004 (which includes the hurricane related samples of September 3-4) to October 25, 2004, the system shows the ability to recover in a relatively short time period. This is also supported by the sustenance of performance during the numerous shut downs over the POR. The performance of the system following Hurricane Frances and Jeanne is noted in Figure 5-1. Following a release of nutrients during the week of the hurricane, there was some recovery after re-start on September 14, 2004. After Hurricane Jeanne, the system showed recovery by the week ending October 25, 2004.The indication is that algal growth recovery is rather rapid. After the two power outages, no effort was made to remove the necrotic algae from the floway prior to restart. If this had been done, it is possible that the rate and extent of recovery would have been improved. However, considering the magnitude of these events, it can be said with confidence that ATS™ system are resilient, and capable of returning to full performance in a short period after extensive dry-down. Therefore, it would not be unreasonable to consider, where appropriate, a system that would function over a portion of the year, while being retired for the remainder. This might work well where seasonal allocations apply, or where annual load removal requirements can be accomplished during the growing season.